

Coplanar Capacitively Coupled Probe Fed Microstrip Antennas for Wideband Applications

Veeresh G. Kasabegoudar and K. J. Vinoy, *Senior Member, IEEE*

Abstract—The design and analysis of a coplanar capacitive fed microstrip antenna suspended above the ground plane is presented. It is demonstrated that the proposed approach can be used for designing antennas with impedance bandwidth of about 50% and a good gain to operate in various microwave bands. The model of the antenna incorporates the capacitive feed strip which is fed by a coaxial probe using equivalent circuit approach, and matches simulation and experimental results. The capacitive feed strip used here is basically a rectangular microstrip capacitor formed from a truncated microstrip transmission line and all its open ends are represented by terminal or edge capacitances. The error analysis was carried out for validity of the model for different design parameters. The antenna configuration can be used where unidirectional radiation patterns are required over a wide bandwidth.

Index Terms—Coplanar capacitive feed, microstrip antennas, wideband and input impedance.

I. INTRODUCTION

MICROSTRIP antennas are suitable for modern broadband applications because of their desirable characteristics [1]–[3]. Although microstrip antennas in their basic form exhibit limited bandwidth, it has been shown by several researchers that the bandwidth can be significantly improved by altering the basic geometry and/or feed or by using impedance matching techniques [2]. However most of these geometries employ stacked multiple metal/dielectric layers [4], or use modified probe shape (L-, T-, or meander-shaped probes) [5]–[7], which elude the primary advantages of microstrip antennas such as ease of fabrication and assembling [8].

On the other hand, the antenna reported in [3] is a single layer coplanar capacitive fed wideband microstrip antenna. This antenna is simple to fabricate and assemble, and the 28% bandwidth reported there could be enhanced by optimizing the dimensions of feed strip and its placement with respect to the radiator patch [8]. Radiation patterns of this antenna with bandwidth of almost 50% can be improved by modifying the edge of the

radiator patch close to the feed strip [9]. The maximum bandwidth can be achieved for this antenna with an overall substrate height of about $0.16 \lambda_0$ [8]. In the above geometries, the antenna has a unidirectional radiation pattern because of the presence of the ground plane. The capacitive feed strip placed along one of the radiating edges of the patch compensates for the probe inductance. This approach for compensating probe inductance is widely known [10], but the impedance bandwidth of the antenna configuration in the present work is significantly higher than previously reported [3], [10].

Input impedance of microstrip antennas plays a major role in determining the matching between antenna terminals and transmission lines. Extensive studies have been reported in the literature on input impedance calculations of microstrip antennas [11]–[22]. A few of these studies include transmission line model [11], cavity model [12], moment method solutions [13]–[17], equivalent circuit (extracted from cavity model i.e., treating volume below the patch as a cavity) approaches [18]–[21], some of which involve solving complicated integrals. An equivalent circuit based approach provides a clear physical insight into the operation of the antenna. The equivalent circuit approaches reported in [18]–[21] are simple and reasonably accurate but these consider that the probe feed is directly connected to the radiator patch geometries. The impedance analysis of coplanar capacitive fed wideband microstrip antenna has been reported by [22] based on full wave analysis. However the suggested method involves numerically intensive calculations for the basic antenna geometry as mentioned above.

In this paper we present the design, optimization, and analysis of input impedance of coplanar capacitive fed wideband microstrip antennas. Input impedance analysis presented here is based on equivalent circuit approach which also incorporates the probe feed connected outside the radiator patch into the complete model. The model developed here is simple to analyze and suitable for CAD implementation. The basic geometry of the antenna and its optimization are presented in Section II. Input impedance analysis of the antenna is presented in Section III. This is followed by experimental validation and conclusions in Sections IV and V, respectively.

II. ANTENNA GEOMETRY AND ITS OPTIMIZATION

The basic geometry of the antenna is shown in Fig. 1 [8] and optimized dimensions are listed in Table I. The configuration is basically a suspended microstrip antenna in which radiating patch and the feed strip are placed above the substrate of thickness “ h ” mm. A long pin SMA connector is used to connect the feed strip which capacitively couples the energy to a radiating patch. The detailed parametric studies have been reported

Manuscript received March 19, 2009; revised November 12, 2009; accepted April 08, 2010. Date of publication July 01, 2010; date of current version October 06, 2010.

V. G. Kasabegoudar is with the Electronics and Telecommunication Engineering Department, College of Engineering, Ambajogai-431517, India (e-mail: veereshgk2002@rediffmail.com).

K. J. Vinoy is with the Microwave Laboratory, Department of Electrical Communication Engineering, Indian Institute of Science, Bangalore 560 012, India (e-mail: kjvinoy@ieee.org).

Color versions of one or more of the figures in this paper are available online at <http://ieeexplore.ieee.org>.

Digital Object Identifier 10.1109/TAP.2010.2055781

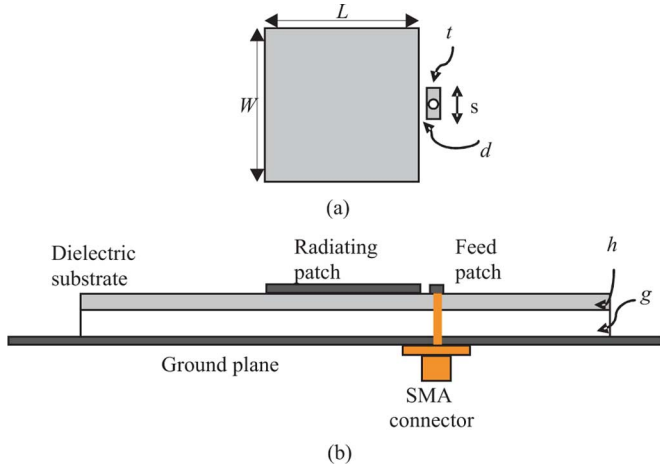


Fig. 1. Basic geometry of coplanar capacitive fed UWB microstrip antenna. (a) Top view. (b) Cross sectional view.

TABLE I
DIMENSIONS FOR THE ANTENNA DESIGNED FOR 5.9 GHz

Parameter	Value
Length of the radiator patch (L)	15.5 mm
Width of the radiator patch (W)	16.4 mm
Length of the feed strip (s)	3.7 mm
Width of the feed strip (t)	1.2 mm
Separation of feed strip from the patch (d)	0.5 mm
Air gap between substrates (g)	6.0 mm
Relative dielectric constant (ϵ_r)	3.0
Thickness of substrate (h)	1.56 mm

earlier [8], [9] for the optimization of this geometry. In this section, we briefly discuss the effect of key design parameters on the antenna performance. These include air gap (g), separation between feed strip and the radiator patch (d), and the length (t) and width (s) (feed strip dimensions). The substrate used for antenna fabrication is a RO3003 with dielectric constant = 3, loss tangent = 0.0013 and thickness $h = 1.56$ mm. All parameters are optimized using IE3D which is a method of moments (MoM) based electromagnetic (EM) software.

The basic patch design starts from the selection of center frequency of the band of operation. For demonstration purpose 5.9 GHz is chosen in the present study. Radiator patch dimensions can be calculated from standard design expressions after making necessary corrections for the suspended ($g + h$) dielectric [1], [23]. These corrections incorporate the total height above the ground and effective dielectric constant of the suspended microstrip [24]. It has been shown that the impedance bandwidth of the antenna may be maximized by using the design expression

$$g \cong 0.16\lambda_0 - h\sqrt{\epsilon_r}. \quad (1)$$

Where g is the height of the substrate above the ground, and h and ϵ_r are the thickness and dielectric constant of the substrate respectively. However, it should be noted that this equation enables us to predict the initial value but the final optimum value would be within $\pm 10\%$ of this [8].

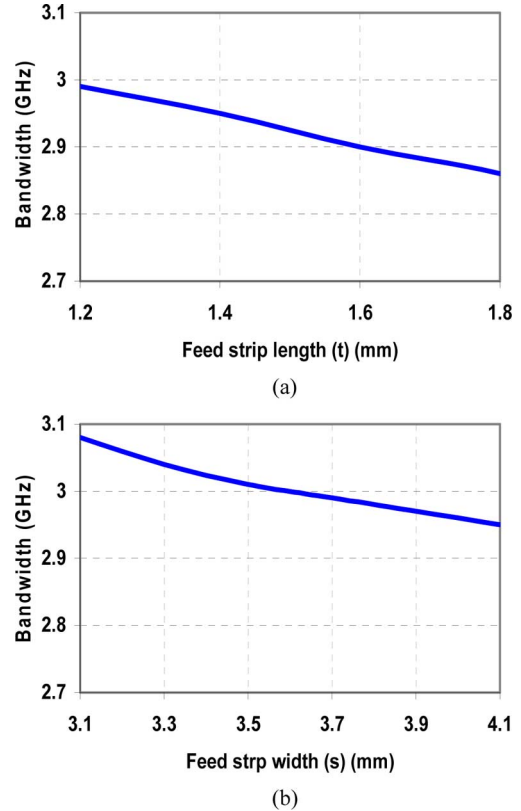


Fig. 2. Effect of feed strip dimensions on impedance bandwidth for an antenna designed to operate at 5.9 GHz as the center frequency. (a) Feed strip length versus bandwidth. (b) Feed strip width versus bandwidth.

As an example, the air gap g was varied from 5.0 mm to 7.5 mm to study its effect on the impedance bandwidth. It can be seen from Table II that the optimum bandwidth solution (set of key design parameters) is not unique and for each air gap value, any of the key design parameters can be used to maximize the antenna bandwidth. For example when air gap is equal to 5.5 mm, there are two possible sets of parameters to get the best possible BW of 3.07 GHz for this height. From these studies, the optimum air gap is found to be 6.0 mm for an antenna operating with a center frequency of 5.9 GHz. However it should be noted that the air gap of 6.0 mm is optimum only for the present operating band and dielectric sheet properties used. Hence the optimum height above ground plane (g) should be recalculated with the help of (1) as discussed above. This is illustrated by considering some arbitrary frequencies (2.0, 4.5, 8.0 and 10.0 GHz) on either side of the present 5.9 GHz. Boresight gain and efficiency for the corresponding center frequency of the operating band for each case are listed in Table II. From Table III it can be seen that nearly 50% bandwidth can be obtained for almost all frequencies considered from the proposed design except for 2.0 GHz case for which the BW is 46%.

For small variations in dielectric constant of the suspended substrate the effective dielectric properties would remain largely unaffected and hence the bandwidth. However there could be a shift in center frequency due to the change in feed strip reactance. A similar effect is also observed with the variation in the thickness of the dielectric layer (h).

TABLE II
OPTIMIZATION OF AIR GAP USING DIFFERENT KEY DESIGN PARAMETERS AND OTHER PARAMETERS ARE AS LISTED IN THE TABLE I

Air gap (g) (mm)	Dimensions of feed strip (txs) (mm) ²	Separation (d) of feed strip (mm)	Bandwidth (GHz)	Boresight gain at the center frequency of the operating band (dB)	Efficiency at the center frequency of the operating band (%)
5.0	2.0x5.5	0.2	2.71	6.62	88.53
5.5	1.8x3.7	0.5	3.01	6.66	98.23
5.5	1.2x4.1	0.5	3.07	6.69	98.27
5.5	1.2x3.8	0.1	3.07	5.91	89.79
6.0	1.2x3.7	0.5	2.99	6.74	98.14
6.0	1.6x2.8	0.5	3.09	6.90	98.21
6.5	1.2x3.7	0.5	2.82	6.89	97.48
7.0	1.2x3.7	0.5	2.66	5.93	87.93
7.5	1.2x3.7	0.5	2.46	5.47	87.65

TABLE III
SCALING OF ANTENNA FOR DIFFERENT CENTER FREQUENCIES WITH THEIR OPTIMUM DIMENSIONS

Design center frequency (GHz)	Dimensions of radiator patch (LxW) (mm) ²	Initial air gap (g) by (1) (mm)	Optimum air gap (g) (mm)	Dimensions of feed strip (txs) (mm) ²	Percentage Bandwidth
2.0	42.8x53.0	21.3	19.2	1.8x6.2	46.0
4.5	21.0x26.5	7.96	7.8	1.2x5.0	50.3
5.9	15.5x16.4	5.43	5.5	1.2x3.7	50.4
8.0	10.0x13.2	3.30	3.5	1.2x3.7	54.4
10.0	7.8x10.6	2.10	2.25	1.2x3.7	58.2

Finally, the effect of feed strip dimensions on impedance bandwidth was investigated. These two dimensions (t and s) control the reactive part of the antenna's input impedance. It can be noticed from Fig. 2 that impedance bandwidth decreases with the increase in t or s . In other words, the bandwidth lost in increasing one parameter can be regained by decreasing the other. For example changing " t " from 1.2 mm to 1.8 mm results in the reduction of bandwidth from 2.99 GHz to 2.80 GHz, which can be restored by reducing the dimension " s " from 4.1 mm to 3.1 mm (Fig. 2(b)). However it should be noted that use of lower dimensions ($t < 1.2$ mm) may pose difficulty in soldering the SMA probe pin while higher values ($s > 4.1$ mm) cause feed strip radiations to disturb the radiation field [8]. For further details on parametric studies, our earlier works [8], [9] may be useful.

III. EQUIVALENT CIRCUIT MODELING

To find the input impedance of the antenna, analysis is made in following paragraphs.

A. Radiator Patch

The equivalent model of a rectangular microstrip antenna is basically a parallel tuned circuit for the antenna operating in the fundamental mode [1]. For the fundamental mode of operation its equivalent circuit consists of well known parallel combination of RLC elements. However it should be noted that for

DC and extremely high frequency operations, a capacitor and an inductor, respectively, can be placed in series with the equivalent circuit of fundamental mode. The radiating patch may be treated as an edge fed microstrip antenna for calculating the patch equivalent capacitance (C_{patch})

$$C_{patch} = \frac{\epsilon_0 \epsilon_{reff} LW}{2(g+h)}. \quad (2)$$

It may be noted that height of the dielectric substrate here is the total height of the geometry including air gap and the effective dielectric constant for the suspended or airdielectric configuration calculated from the equations given in [24]. In the present case, the antenna was designed to operate in the TM_{10} mode and other values (L_{patch} and R_{patch}) of the patch equivalent can be calculated from equations given in [23].

B. Feed Section

As discussed in earlier sections, in the present geometry (Fig. 1), the coaxial probe is not directly connected to the radiator patch instead it is connected to a small rectangular strip placed near the radiator patch which excites it by capacitive coupling. Feed strip can be treated as a rectangular microstrip capacitor as its dimensions are much smaller in comparison with the wavelength of operation. It can also be considered as an abruptly terminated microstrip line and all of its sides (open ends) that can be represented by terminal capacitances. The

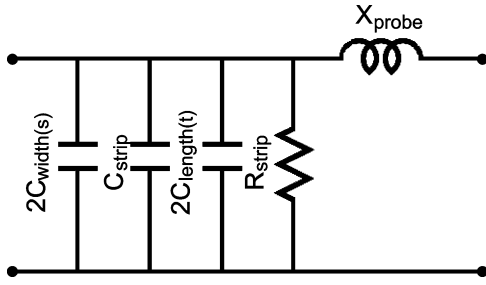


Fig. 3. Equivalent circuit of probe with feed strip.

parallel plate capacitance of the feed strip (C_{strip}) is given in (3)

$$C_{strip} = \frac{\epsilon_0 \epsilon_{reff} s \times t}{(g+h)}. \quad (3)$$

It may be noted that the area of the strip is much smaller than the patch. The perimeter to area ratio is much larger in this case. Hence the fringing capacitances from the edges may be significant in this case. These capacitances, often known as terminal capacitances of the line, can be calculated from [20]:

$$C_{length(t)} = \frac{t}{2} \left[\frac{Z_{air}}{c_0 Z_{sub}^2} - \frac{\epsilon_0 \epsilon_{reff} s}{(g+h)} \right] \quad (4)$$

$$C_{width(s)} = \frac{s}{2} \left[\frac{Z_{air}}{c_0 Z_{sub}^2} - \frac{\epsilon_0 \epsilon_{reff} t}{(g+h)} \right]. \quad (5)$$

In (4) and (5) and, Z_{air} and Z_{sub} are microstrip line impedances in air and substrate medium. A factor of 2 is used here to include opposite sides (Fig. 3). The dissipation and radiation losses from the feed strip are modeled with a resistance R_{strip} . At lower frequencies radiation losses from the feed strip can be neglected. However with the increase in the operating frequency, radiation losses should be taken into account. The strip resistance can be calculated similar to the patch equivalent resistance.

The probe feed can be represented by an inductive reactance element (X_{probe}) in series with the feed strip equivalent circuit [20]. The probe reactance can be calculated from [20], [21]

$$X_{probe} = \frac{377 f_c (g+h)}{c_0} \log_e \left(\frac{c_0}{\pi f_c d_0 \sqrt{\epsilon_{re}}} \right). \quad (6)$$

Where d_0 is the probe diameter, f_c is the operating frequency; c_0 is the velocity of wave through a free space, $(g+h)$ is the total height of mixed air substrate combination, and ϵ_{re} is the equivalent dielectric constant of the composite air-dielectric medium and can be calculated by

$$\epsilon_{re} = \frac{\epsilon_r \left(1 + \frac{g}{h}\right)}{1 + \epsilon_r \left(\frac{g}{h}\right)}.$$

Based on the above, the equivalent model of the feed is shown in Fig. 3. This circuit models the effects in the region below the feed strip.

C. Separation Between Radiator Patch and Feed Strip

The separation between radiator patch and the feed strip is essentially an asymmetrical gap i.e., two conductors of unequal

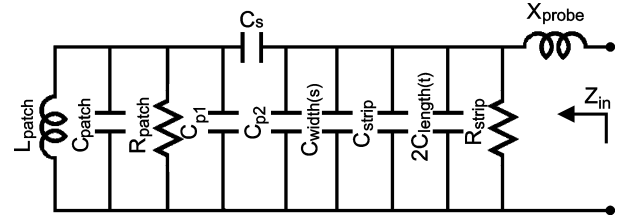


Fig. 4. Complete circuit model of antenna shown in Fig. 1.

width, separated by a short distance (d). The separation between the radiator patch and feed strip can be modeled by the π -network (C_{p1} , C_s , and C_{p2} shown in Fig. 4) given in [25]. Two parallel capacitors (C_{p1} and C_{p2}) represent the terminal capacitances of the two microstrip sections and the series capacitance (C_s) represents the gap. These capacitances can be calculated by a rigorous spectral domain method [25] after making necessary corrections for two layer air dielectric medium

$$C_{p1} = C_{width(s)} \times \frac{T_2 + T_4}{T_2 + 1} \quad (7)$$

$$C_{p2} = C_{patch_edge} \times \frac{T_2 + T_3}{T_2 + 1} \quad \text{and} \quad (8)$$

$$C_s = \left(\frac{h}{g+h} \right)^{0.2257} \times 0.5 \times 10^{-12} \times (g+h) T_1 \times \exp \left(-1.86 \times \frac{d}{(g+h)} \right) \times \left[1 + 4.19 \left(1 - \exp \left(-0.785 \sqrt{\frac{(g+h)}{s}} \times \frac{W}{s} \right) \right) \right]. \quad (9)$$

In (7)–(9) [25],

$$T_1 = 0.04598 \left\{ 0.03 + \left(\frac{s}{(g+h)} \right)^{T_s} \right\} \times (0.272 + \epsilon_{reff} \times 0.07) \quad (10)$$

$$T_2 = 0.107 \left(\frac{s}{(g+h)} + 9 \right) \left(\frac{d}{(g+h)} \right)^{3.23} + 2.09 \left(\frac{d}{(g+h)} \right)^{1.05} \left[\frac{1.5 + 0.3 \left(\frac{s}{(g+h)} \right)}{1 + 0.6 \left(\frac{s}{(g+h)} \right)} \right] \quad (11)$$

$$T_3 = \exp \left[-0.5978 \left(\frac{W}{s} \right)^{1.35} \right] - 0.55 + T_{31} \quad (12)$$

$$T_4 = \exp \left[-0.5978 \left(\frac{s}{W} \right)^{1.35} \right] - 0.55 + T_{41} \quad (13)$$

$$T_5 = \frac{1.23}{\left[1 + 0.12 \left\{ \left(\frac{W}{s} \right) - 1 \right\}^{0.97} \right]}. \quad (14)$$

Some additional correction factors have been added to few terms of these equations based on data obtained from a number of cases studied. However it should be noted that, these correction factors are required only outside the parametric range ($1 \leq s/W \leq 3$, and $0.2 \leq d/(g+h) \leq \infty$) defined in [25] and for suspended configurations. For example in the present case, $s/W < 1$ (0.22) and $d/(g+h) < 0.2$ (0.066) are outside the

range mentioned above and hence need corrections. With these corrections, the model works for different values of feed strip dimensions considered in [8] to obtain best possible bandwidth for this antenna ($\sim 50\%$). In T_3 and T_4 , T_{31} and T_{41} are the correction factors for suspended substrates, whose values are defined as

$$T_{31} = T_{41} = 0 \text{ for } g = 0.$$

And for $g > 0$

$$T_{31} = \left[-0.73 + \left(1.05 \left(\frac{W}{s} \right)^{0.88} - 3.892 \right) \times \exp \left(-8.23 \left(\frac{W}{s} \right)^{0.88} \right) \right] \quad (15)$$

$$T_{41} = \left[1.55 - \left(13.61 \left(\frac{t}{W} \right)^{0.88} - 1.361 \right) \times \exp \left(-4.793 \left(\frac{t}{W} \right)^{0.88} \right) - 0.1 \times \exp \left(- \left(13.61 \left(\frac{t}{W} \right)^{0.88} - 1.361 \right) \right) \right]. \quad (16)$$

In all above expressions, the substrate height h is replaced by the total height to include air-dielectric medium ($g + h$). In (8), the static edge capacitance of the radiator patch capacitance can be computed from

$$C_{patch_edge} = \frac{W}{2} \left[\frac{Z_{air}}{c_0 Z_{sub}^2} - \frac{\epsilon_0 \epsilon_{reff} L}{(g + h)} \right]. \quad (17)$$

In (17), Z_{air} and Z_{sub} are microstrip line impedances in air and substrate medium respectively. It should be noted that the dynamic radiating edge capacitance of the patch is equal to its static edge capacitance as the antenna is designed to operate in the TM_{10} mode. The strip width fringing capacitance (C_{width}) in (7) can be calculated as explained in Section III-B.

D. Complete Equivalent Circuit

The complete circuit after combining all individual parts of entire geometry developed in the above paragraphs is shown in Fig. 4.

The input impedance of the complete antenna geometry shown in Fig. 4 can be calculated from

$$Z_{in} = \left[\frac{1}{Z_{patch} + j\omega C_{p1}} \right]^{-1} + \frac{1}{j\omega C_s} + \left[\frac{1}{Z_{feed_strip} + j\omega C_{p2}} \right]^{-1} + jX_{probe}. \quad (18)$$

In (18), Z_{patch} is the input impedance of patch equivalent and Z_{feed_strip} is the input impedance of feed strip.

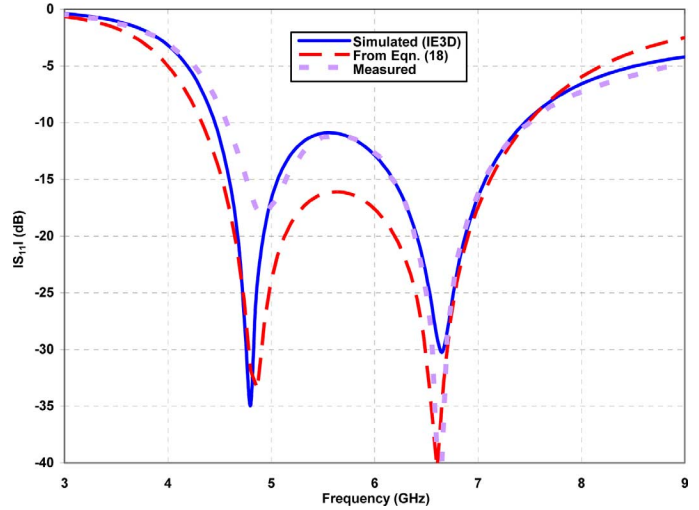


Fig. 5. S_{11} characteristics obtained from different techniques for the antenna shown in Fig. 1.

IV. VALIDATION OF THE MODEL AND DISCUSSIONS

Above designed prototype with dimensions given in Table I was fabricated and its characteristics (S_{11} (dB) (input reflection coefficient), gain and radiation patterns) were measured. The input impedance model given by (18) was implemented in MATLAB. The S_{11} characteristics obtained from simulation, measurement and our model are compared in Fig. 5. It can be noticed from Fig. 5 that model is in good agreement with the simulated and measured results. For other values of feed strip dimensions, the S_{11} characteristics from the model do not deviate much with the simulated results obtained from the IE3D. All geometries were simulated with the probe diameter of 1.4 mm of a commercially available SMA connector. The substrate used for all the simulations, analysis and fabrication of the antenna is Roger's made RO3003 with dielectric constant of 3.0, loss tangent of 0.0013 and thickness of 1.56 mm.

Tables IV and V show the performance for different sets of values of feed strip length (t) from 1.2 mm to 1.8 mm and width (s) from 3.1 mm to 4.1 mm and found good matching with the simulated results. The model was tested further for bands of frequencies (L, S, C, and X) as the microstrip antenna is redesigned for almost any frequency by appropriate scaling in Table VI. The frequencies chosen within these bands are 2, 4.5, 5.9, 8, and 10 GHz as demonstrated in [8]. For all these designs, we found good match between the simulated and the calculated S_{11} characteristics. In Tables IV–VI, a comparison of frequency deviation between the measured and computed values of the two resonant frequencies of antenna is given. The resonant frequencies (f_1 and f_2) correspond to the peak negative values of the S_{11} characteristics. From these studies, it can be noted that the total relative percentage error does not exceed 3.5% in all cases considered (Tables IV–VI). Since the error is much smaller than the bandwidth, we conclude that the percentage of error is acceptably low.

Radiation patterns were measured in an anechoic chamber. Comparisons of simulated and measured radiations patterns of E and H plane patterns at the start, center, and end frequencies

TABLE IV
ERROR ANALYSIS FOR TWO RESONANT FREQUENCIES IN THE S_{11} BAND (-10 dB) WITH FEED STRIP WIDTH ($s = 3.7$ mm) CONSTANT

t (mm)	f_1			f_2		
	Calculated from our model (GHz)	Simulated (IE3D) (GHz)	%Error	Calculated from our model (GHz)	Simulated (IE3D) (GHz)	%Error
1.2	4.86	4.80	1.25	6.60	6.65	-0.75
1.4	4.80	4.82	-0.41	6.66	6.64	0.30
1.6	4.80	4.82	-0.41	6.60	6.54	0.91
1.8	4.80	4.82	-0.41	6.53	6.50	0.46

TABLE V
ERROR ANALYSIS FOR TWO RESONANT FREQUENCIES IN THE S_{11} BAND (-10 dB) WITH FEED STRIP LENGTH ($t = 1.2$ mm) CONSTANT

s (mm)	f_1			f_2		
	Calculated from our model (GHz)	Simulated (IE3D) (GHz)	%Error	Calculated from our model (GHz)	Simulated (IE3D) (GHz)	%Error
3.1	4.86	4.84	0.42	6.86	6.77	1.33
3.3	4.86	4.84	0.42	6.79	6.76	0.45
3.5	4.86	4.84	0.42	6.67	6.66	0.15
3.7	4.86	4.80	1.25	6.60	6.65	-0.75
4.2	4.73	4.76	-0.63	6.34	6.51	-2.61

TABLE VI
ERROR ANALYSIS FOR TWO RESONANT FREQUENCIES IN THE S_{11} BAND (-10 dB) FOR DIFFERENT BANDS OF FREQUENCIES

Designed Frequency (GHz)	f_1			f_2		
	Calculated from our model (GHz)	Simulated (IE3D) (GHz)	%Error	Calculated from our model (GHz)	Simulated (IE3D) (GHz)	%Error
2.0	1.84	1.81	1.65	2.43	2.36	2.96
4.5	3.77	3.82	-1.30	5.03	5.00	0.60
5.9	4.86	4.80	1.25	6.60	6.65	-0.75
8.0	6.88	6.78	1.47	9.05	8.97	0.89
10.0	8.7	8.61	1.04	11.0	11.28	-2.48

of the useful frequency band are shown in Fig. 6. These emphasize the unidirectional nature of the radiations. It may be noted that the H-plane patterns are symmetrical throughout the band of operation whereas E-plane patterns are symmetrical at lower frequencies and the degree of asymmetry increases at the higher end of the operating band. Furthermore, these also indicate minor beam squinting and increased cross polarization levels. These may be attributed to the excitation of unwanted higher order modes and/or spurious direct radiations from the feed [26]–[29]. Approaches suggested to address these problems are based on modifying the probe feed of the patch such as by employing a dual feed arrangement with 180° phase shift [26], or a balanced feeding technique [27]. In a separate effort,

the geometry of the presently used capacitively coupled patch has been modified to achieve symmetrical E-plane radiation patterns across the band of operation [9].

However, it can be noted that the measured radiation patterns show more than -20 dB cross polarization level in the boresight direction and a comfortable -15 dB back lobe radiation levels. Comparisons of simulated and measured gain versus frequency characteristics of the antenna are plotted in Fig. 7. The gain was measured by comparison (three antennas) method. The gain is above 6 dBi at the center of the operating band.

From all above discussions, it can be noted that all results (simulated and calculated from equations presented in this paper), fairly agree with the measured results.

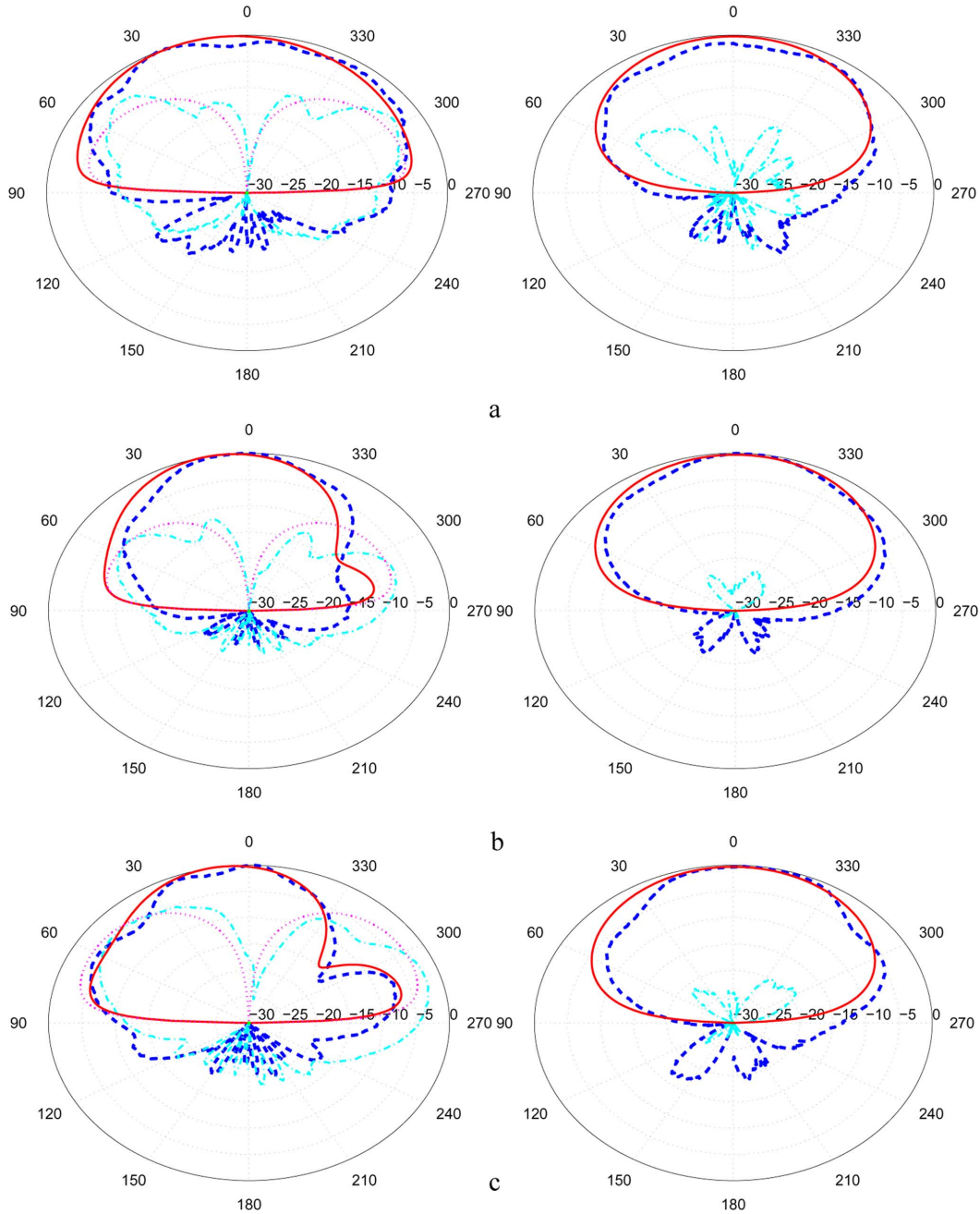


Fig. 6. Radiation patterns comparisons of antenna shown in Fig. 1. (Left-hand side: E-plane patterns and right-hand side: H-plane patterns). Solid line: Simulated co-polarizations; Dashed line: Measured co-polarizations; Dotted Line: Simulated cross polarizations; Dashed-dotted line: Measured cross-polarizations. Note: H-cross (simulated) cannot be seen in patterns as it is well below -30 dB. (a) E and H-plane patterns at 4.5 GHz. (b) E and H-plane patterns at 6.0 GHz. (c) E and H-plane patterns at 7.5 GHz.

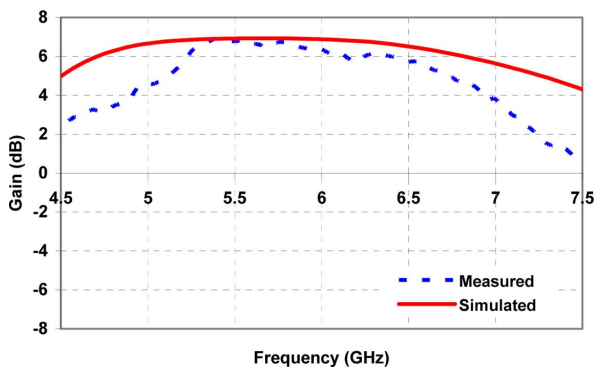


Fig. 7. Gain versus frequency plots.

V. CONCLUSIONS

A coplanar capacitively coupled probe fed microstrip antenna suitable for wideband applications has been presented. After presenting the basic configuration, an equivalent circuit based approach to calculate the input impedance is discussed. This unified model predicts the input impedance of the antenna, including the effects of the feed strip and the probe pin, over a wide range of frequencies. Input impedance and S_{11} characteristics obtained using the developed equations are found to be in good agreement with the IE3D simulated and experimental results. Some of the expressions for the constituent models have been modified to suit the proposed antenna configuration. With this

approach, conformal wideband antennas have been designed with different center frequencies from 2 GHz to 10 GHz and all of these showed nearly similar radiation performance.

REFERENCES

- [1] R. Garg, P. Bhartia, I. Bahl, and A. Ittipiboon, *Microstrip Antenna Design Handbook*. Norwood, MA: Artech House, 2001.
- [2] G. Kumar and K. P. Ray, *Broadband Microstrip Antennas*. Norwood, MA: Artech House, 2003.
- [3] G. Mayhew-Ridgers, J. W. Odendaal, and J. Joubert, "Single-layer capacitive feed for wideband probe-fed microstrip antenna elements," *IEEE Trans. Antennas Propag.*, vol. 51, pp. 1405–1407, 2003.
- [4] D. M. Kokotoff, J. T. Aberle, and R. B. Waterhouse, "Rigorous analysis of probe fed printed annular ring antennas," *IEEE Trans. Antennas Propag.*, vol. 47, pp. 384–388, 1999.
- [5] B. L. Ooi and I. Ang, "Broadband semicircle fed flower-shaped microstrip patch antenna," *Electron. Lett.*, vol. 41, no. 17, 2005.
- [6] C. L. Mak, K. F. Lee, and K. M. Luk, "A novel broadband patch antenna with a T-shaped probe," *Proc. Inst. Elect. Eng., Microw., Antennas Propag.*, vol. 147, pp. 73–76, 2000.
- [7] H. W. Lai and K. M. Luk, "Wideband stacked patch antenna fed by meandering probe," *Electron. Lett.*, vol. 41, no. 6, 2005.
- [8] V. G. Kasabegoudar, D. S. Upadhyay, and K. J. Vinoy, "Design studies of ultra wideband microstrip antennas with a small capacitive feed," *Int. J. Antennas Propag.*, vol. 2007, pp. 1–8.
- [9] V. G. Kasabegoudar and K. J. Vinoy, "A wideband microstrip antenna with symmetric radiation patterns," *Microw. Opt. Technol. Lett.*, vol. 50, no. 8, pp. 1991–1995, 2008.
- [10] P. S. Hall, "Probe compensation in thick microstrip patches," *Electron. Lett.*, vol. 23, pp. 606–607, 1987.
- [11] A. K. Bhattacharjee, S. R. B. Chaudhuri, A. Mukherjee, D. R. Poddar, and S. K. Chowdhury, "Input impedance of rectangular microstrip antennas," *Proc. Inst. Elect. Eng. Pt. H.*, vol. 135, no. 5, pp. 351–352, 1988.
- [12] Y. T. Lo, D. Solomon, and W. F. Richards, "Theory and experiment on microstrip antennas," *IEEE Trans. Antennas Propag.*, vol. 27, pp. 137–145, 1979.
- [13] E. H. Newman and T. Pravit, "Analysis of microstrip antennas using moment methods," *IEEE Trans. Antennas Propag.*, vol. 29, pp. 47–53, 1981.
- [14] M. D. Deshpande and M. Bailey, "Input impedance of microstrip antennas," *IEEE Trans. Antennas Propag.*, vol. 30, pp. 645–650, 1982.
- [15] D. M. Pozar, "Input impedance and mutual coupling of rectangular microstrip antennas," *IEEE Trans. Antennas Propag.*, vol. 30, pp. 1191–1196, 1982.
- [16] J. P. Damiano, J. Bennegouche, and A. Papiernik, "Study of multilayer microstrip antennas with radiating elements of various geometries," *Proc. Inst. Elect. Eng. Pt. H.*, vol. 137, no. 3, pp. 163–170, 1990.
- [17] J. P. Damiano and A. Papiernik, "Survey of analytical and numerical models for probe-fed microstrip antennas," *Proc. Inst. Elect. Eng., Microw. Antennas Propag.*, vol. 141, no. 1, pp. 15–22, 1994.
- [18] V. K. Pandey and B. R. Vishvakarma, "Analysis of an E-shaped patch antenna," *Microw. Opt. Technol. Lett.*, vol. 49, no. 1, pp. 4–7, 2007.
- [19] J. A. Ansari and R. B. Ram, "Analysis of a compact and broadband microstrip patch antenna," *Microw. Opt. Technol. Lett.*, vol. 50, no. 8, pp. 2059–2063, 2008.
- [20] F. Abboud, J. P. Damiano, and A. Papiernik, "Simple model for the input impedance of the coax-feed rectangular microstrip patch antenna for CAD," *Proc. Inst. Elect. Eng.*, vol. 135, no. 5, pp. 323–326, 1988.
- [21] A. K. Verma, N. V. Tyagi, and D. Chakraverty, "Input impedance of probe fed multilayer rectangular microstrip patch antenna using the modified Wolff model," *Microw. Opt. Technol. Lett.*, vol. 31, no. 3, pp. 237–239, 2001.
- [22] G. Mayhew-Ridgers, J. W. Odendaal, and J. Joubert, "Efficient full-wave modeling of patch antenna arrays with new single-layer capacitive feed probes," *IEEE Trans. Antennas Propag.*, vol. 53, pp. 3219–3228, 2005.
- [23] I. J. Bahl and P. Bhartia, *Microstrip Antennas*. Boston, MA: Artech House, 1980.
- [24] J. M. Schellenberg, "CAD models for suspended and inverted microstrip," *IEEE Trans. Microw. Theory Tech.*, vol. 43, no. 6, pp. 1247–1252, 1995.
- [25] M. Kirschning, R. H. Jansen, Jansen, and N. H. L. Koster, "Measurement and computer aided modeling of microstrip discontinuities by an improved resonator method," *IEEE MTT-S Digest*, pp. 495–497, 1983.
- [26] C. H. K. Chin, Q. Xue, and H. Wong, "Broadband patch antenna with a folded pair as a differential feeding scheme," *IEEE Trans. Antennas Propag.*, vol. 55, pp. 2461–2467, 2007.
- [27] Z. N. Chen and M. Y. W. Chia, "Experimental study on radiation performance of probe-fed suspended plate antennas," *IEEE Trans. Antennas Propag.*, vol. 51, pp. 1964–1971, 2003.
- [28] X. N. Low, Z. N. Chen, and W. K. Toh, "Ultrawideband suspended plate antenna with enhanced impedance and radiation performance," *IEEE Trans. Antennas Propag.*, vol. 56, pp. 2490–2495, 2008.
- [29] C. Y. D. Sim, C. C. Chang, and J. S. Row, "Dual feed dual polarized patch antenna with low cross polarization and high isolation," *IEEE Trans. Antennas Propag.*, vol. 57, pp. 3405–3409, 2009.



Veeresh G. Kasabegoudar received the Bachelor's degree from Karnatak University Dharwad, India, the Masters degree from the Indian Institute of Technology (IIT) Bombay, India, and the Ph.D. degree from the Indian Institute of Science (IISc), Bangalore, in 1996, 2002, and 2009, respectively.

From 1996 to 2000, he worked as a Lecturer in the Electronics and Telecommunication Engineering Department, College of Engineering, Ambajogai, India, where, from 2002 to 2006, he worked as an Assistant Professor and, since 2008, he has been a Professor and Dean of Research and Development. He has published over 15 papers in technical journals and conferences. His research interests include microstrip and CPW fed antennas, and microwave filters.



K. J. Vinoy (M'02–SM'06) received the Bachelor's degree from the University of Kerala, India, the Masters degree from Cochin University of Science and Technology, Cochin, India, and the Ph.D. degree from the Pennsylvania State University, University Park, in 1990, 1993, and 2002, respectively.

From 1994 to 1998, he worked in various positions at the National Aerospace Laboratories, Bangalore, India, where he was attached to the Computational Electromagnetics Group. He was a Research Assistant at the Center for the Engineering of Electronic and Acoustic Materials and Devices (CEEAMD) at the Pennsylvania State University, from 1999 to 2002. He continued there for Postdoctoral research until 2003. Since 2003, he has been with the Department of Electrical Communication Engineering, Indian Institute of Science, Bangalore, where he is currently an Associate Professor. His research interests cover several aspects of microwave engineering including, microwave antennas, microwave circuits, metamaterials and RF MEMS. He has published over 100 papers in technical journals and conferences. He has also published three books: *Radar Absorbing Materials: From Theory to Design and Characterization* (Kluwer, 1996), *RF MEMS and their Applications* (Wiley, 2002), and *Smart Material Systems and MEMS: Design and Development Methodologies* (Wiley, 2006). He is serving on the editorial board of the *Journal of the Indian Institute of Science*.

Prof. Vinoy is currently the Chairman of the IEEE joint MTT/AP Societies Bangalore Chapter.